Knot probability for lattice polygons in confined geometries

1994 J. Phys. A: Math. Gen. 27 347

(http://iopscience.iop.org/0305-4470/27/2/019)

J. Phys. A: Math. Gen. 27 (1994) 347–360. Printed in the UK

Knot probability for lattice polygons in confined geometries

M C Tesi†, E J Janse van Rensburg‡, E Orlandini† and S G Whittington†
† Department of Chemistry, University of Toronto, Toronto, Canada M5S 1A1
‡ Department of Mathematics and Statistics, York University, Downsview, Ontario, Canada M3J 1P3

Received 27 July 1993, in final form 7 October 1993

Abstract. We study the knot probability of polygons confined to slabs or prisms, considered as subsets of the simple cubic lattice. We show rigorously that almost all sufficiently long polygons in a slab are knotted and we use Monte Carlo methods to investigate the behaviour of the knot probability as a function of the width of the slab or prism and the number of edges in the polygon. In addition we consider the effect of solvent quality on the knot probability in these confined geometries.

1. Introduction

Knots in closed polymer chains are of interest in polymer physics, chemistry, molecular biology and knot theory, and knotting can have an important influence on a number of polymer properties. For instance, the effects of knots on the rheology of polymer networks were investigated by Edwards (1967, 1968), and de Gennes (1984) considered tight knots in polymers and the effect which they have on long-time memory effects in melts of crystallizable linear polymers. In addition, the presence of knots in closed circular DNA can give information about the mechanism of action of enzymes acting on the DNA molecules (Wasserman *et al* 1985, Wasserman and Cozzarelli 1986). In this context knots have been detected in circular DNA, their knot type identified by electron microscopy (Dean and Cozzarelli 1985, Wasserman and Cozzarelli 1991), and the knot probability measured experimentally as a function of the degree of polymerization and the ionic strength (Shaw and Wang 1993).

Ring polymers (such as closed circular DNA) can be modelled as n-step self-avoiding polygons on a regular lattice, and the presence of knots in polygons (and in related models, such as polygons in R^3) has been studied using Monte Carlo methods by a number of workers (Vologodskii *et al* 1974, Michels and Wiegel 1986, Janse van Rensburg and Whittington 1990, Koniaris and Muthukumar 1991). Little is known rigorously, but it has been shown that sufficiently long polygons are knotted with probability one (Sumners and Whittington 1988, Pippenger 1989). These rigorous results have been successively extended to the more general case of graphs embedded in $\mathcal{Z}^3$ (Soteros *et al* 1992) and to the problem of the entanglement complexity of self-avoiding walks (Janse van Rensburg *et al* 1992).

Polymers are often confined to restricted spaces; for instance the presence of histones and other large molecules in the cell-nucleus confines the cellular DNA to reduced spaces, with corresponding effects on the geometrical and topological properties of the DNA. In this paper we consider the effects of such geometrical constraints on the knot probability of ring polymers modelled by polygons in the cubic lattice, in the specific cases where the polygons are confined to a slab or to a prism. (The only previous work in this area, as far

0305-4470/94/020347+14$07.50

as we know, is a paper by Michels and Wiegel (1989) in which they model ring polymers in a thin slab as closed curves in R^2 in which the intersections are chosen randomly to be under- or over-crossings. They find that the knot probability is higher than for polygons in R^3.) In section 2 we present some rigorous results; in particular, we investigate the n-dependence of the knot probability for polygons confined to a slab of the simple cubic lattice. In section 3 we explain the implementation of a Monte Carlo program to simulate polygons in the cubic lattice, and we explore the possibility of using rejection techniques to extract data on the properties of polygons confined to slabs and prisms. We present and discuss the results of some simulations in section 4 and give some brief conclusions and suggestions for future work in section 5.

2. Rigorous results

An *n-step walk* is an ordered sequence $\omega_0, \omega_1, \omega_2, \ldots, \omega_n$ of points of $\mathcal{Z}^3$ such that successive points are unit distance apart; it is an *n-step self-avoiding walk* (which we shall abbreviate to an n-SAW) if these $n+1$ points are all distinct. We call the points $\omega_0, \omega_1, \ldots, \omega_n$ the vertices of the walk, and we consider two walks to be *equivalent* if one is a translate of the other. One is often interested in the properties of n-SAWs to within equivalence, and in this case it is convenient to consider the walks with the first vertex at the origin and to write c_n for the number of such walks.

An *n-step self-avoiding circuit* is an $(n-1)$-SAW whose first and last vertices ω_0 and ω_{n-1} are unit distance apart. If $\omega_0, \omega_1, \omega_2, \ldots, \omega_{n-1}$ are the successive vertices of an n-step self-avoiding circuit, then any cyclic permutation or reflection of a cyclic permutation of the vertices is also an n-step self-avoiding circuit. The equivalence class of $2n$ n-step self-avoiding circuits may be regarded as a single (unlabelled) geometrical object which we call an n-step self-avoiding polygon or simply an n-SAP. Two polygons are equivalent if one is a translate of the other, and we write p_n for the number of inequivalent n-SAPs. An n-SAP is said to be rooted if it contains one labelled vertex which coincides with the origin and, since the root can be chosen in n ways, the number of distinct rooted n-SAPs is np_n. In what follows, we shall use the term *polygon* to denote either n-SAPs or rooted n-SAPs.

Hammersley (1961) has shown that there exists a connective constant $\kappa > 0$ such that

$$p_n = \mathrm{e}^{\kappa n + o(n)} \tag{2.1}$$

and similar techniques, together with the use of a pattern theorem (Kesten 1963), have been used (Sumners and Whittington 1988, Pippenger 1989) to prove that the number p_n^0 of *unknotted* polygons behaves as

$$p_n^0 = \mathrm{e}^{\kappa_0 n + o(n)} \tag{2.2}$$

with $0 < \kappa_0 < \kappa$, so that the probability $P(n)$ that the polygon is a knot goes to unity exponentially rapidly as

$$P(n) = 1 - p_n^0/p_n = 1 - \mathrm{e}^{-\alpha_0 n + o(n)} \tag{2.3}$$

for some positive constant $\alpha_0 = \kappa - \kappa_0$. One concludes that unknotted polygons comprise an exponentially small fraction of all polygons as n tends to infinity. Similar results are valid for various continuum versions of piecewise linear embeddings of circles in R^3 (Diao

1990, Diao *et al* 1993). For related results see also Frisch and Klempner (1970) and Kendall (1979).

In this paper we shall be concerned with knotting of polygons confined to certain subsets of the simple cubic lattice $\mathcal{Z}^3$. We define an *L-slab* as the section graph of $\mathcal{Z}^3$ whose vertex set is the set of vertices of $\mathcal{Z}^3$ with z-coordinate in the range $0 \leqslant z \leqslant L$, and whose edge set is the set of edges of $\mathcal{Z}^3$ incident on two of these vertices. Similarly an *(L_1, L_2)-prism* is the section graph of $\mathcal{Z}^3$ with vertices having y and z coordinates satisfying $0 \leqslant y \leqslant L_1$ and $0 \leqslant z \leqslant L_2$, and with the edges of $\mathcal{Z}^3$ which are incident on two of these vertices. Let $c_n(L)$ be the number of self-avoiding walks, in an L-slab, with n edges and first vertex rooted at the origin. Similarly, let $p_n(L)$ be the number of (unrooted) polygons confined to an L-slab. We regard two polygons as distinct if they can not be superimposed by translation in the x or y directions. We can now prove the analogous result to (2.3) for polygons confined to an L-slab. In order to do this, we note the following lemma.

Lemma 2.1 (Hammersley and Whittington 1985). If $c_n(L)$ is the number of n-step self-avoiding walks in an *L-slab*, the limit

$$\lim_{n\to\infty} n^{-1} \log c_n(L) = \kappa(L) \tag{2.4}$$

exists for all L. Moreover, $\kappa(L)$ is strictly monotonically increasing in L and $\lim_{L\to\infty} \kappa(L) = \kappa$.

We next need to generalize the pattern theorem for walks (Kesten 1963) to walks confined in an L-slab. A Kesten pattern K is a finite self-avoiding walk such that there exists a self-avoiding walk which contains three copies of K. For any $\alpha > 0$ and $\beta > 0$, define a $K_{\alpha,\beta}$ pattern to be any self-avoiding walk ω such that at least three disjoint copies of ω occur on some self-avoiding walk ω^*, where one endpoint of ω^* is the origin, and the other is $(\alpha, \beta, 0)$. In addition, ω^* is completely contained in $D_{\alpha,\beta} = \{(x, y, z) \in Z^3 : 0 \leqslant x \leqslant \alpha, 0 \leqslant y \leqslant \beta, 0 \leqslant z \leqslant L\}$. Then we have the following lemma.

Lemma 2.2. For any $\alpha > 0$ and $\beta > 0$, let P be a $K_{\alpha,\beta}$ pattern, then

$$\limsup_{n\to\infty} n^{-1} \log c_n(\bar{P}, L) = \kappa(\bar{P}, L) < \kappa(L) \tag{2.5}$$

where $c_n(\bar{P}, L)$ is the number of n-step walks in an L-slab which do not contain the pattern P.

The proof of this lemma is similar to the case for walks in a prism (Soteros and Whittington 1989), and we omit the details.

Walks and polygons have the same connective constant, and this is also true when they are confined to an L-slab; indeed the following lemma holds.

Lemma 2.3 (Madras and Slade 1993, p 270). If $p_n(L)$ is the number of *unrooted* polygons in an L-slab then

$$\lim_{n\to\infty} n^{-1} \log p_n(L) = \kappa(L)\,. \tag{2.6}$$

Since deleting an edge cannot create a pattern we have

$$p_n(\bar{P}, L) \leqslant c_{n-1}(\bar{P}, L) \tag{2.7}$$

which, together with (2.5) and (2.6), establishes the following lemma.

Lemma 2.4. If there exists a self-avoiding walk in an L-slab on which a Kesten pattern P occurs then the number of polygons in an L-slab on which P never occurs is such that

$$\lim_{n\to\infty} n^{-1} \log p_n(\bar{P}, L) \leqslant \kappa(\bar{P}, L) < \kappa(L). \qquad (2.8)$$

Lemma 2.4 implies that polygons in an L-slab which do not contain a given pattern P are exponentially rare compared to the total number of polygons in an L-slab.

As a consequence we have the following theorem, which extends the result in (2.3) to the case of self-avoiding polygons in an L-slab.

Theorem 2.1. If we denote by $p_n^0(L)$ the number of unknotted n-SAPs in an L-slab, then the knot probability $P(n, L)$ behaves as

$$P(n, L) = 1 - p_n^0(L)/p_n(L) = 1 - \exp(-\alpha(L)n + o(n)) \qquad (2.9)$$

with $\alpha(L) > 0$.

Proof. We take

$$T = \{-j, -j, k, -j, -j, -k, i, i, j, j, j, -i, k, -i, -i, -k, -j, -j, i, i, k\}$$

where i, j, k are unit vectors in the coordinate directions, as the $K_{\alpha,\beta}$ pattern. This sequence of edges is a *knotted arc* (see Sumners and Whittington (1988) for the technical definition of knotted arc) in a 1-slab, and its presence in a polygon ensures that the polygon will be knotted.

Corollary 2.2. Almost all polygons in an L-slab in Z^3 are knotted.

3. Numerical methods

The configurational and topological properties of polygons subject to geometrical constraints can be studied in two ways. First, one can use an efficient algorithm to generate a realization of a Markov chain defined on the set of n-gons and then use rejection techniques to select the subsequence of polygons in the realization which conform to the constraints. The alternative approach is a direct simulation of polygons in the confined environment. Both these methods have disadvantages. In the first method, one may find that few of the polygons in the realization of the Markov chain satisfy the constraints, which may result in large uncertainties in any averages computed over the realization. In the second case, the problem is more basic: not much is known about Monte Carlo algorithms for polygons or walks in confined environments. In particular, there do not seem to be algorithms available which are ergodic, though we give one example of an efficient and ergodic algorithm for polygons (in a 1-slab) below. In both methods, the essential requirements are the ergodicity of the algorithms and a high efficiency in sampling the relevant state space.

For most of the work reported here we have used the first approach: generating a realization of a Markov chain defined on the set of *all* n-gons, and using rejection techniques to compute averages over polygons satisfying the geometrical constraints. A modification of the 'cut-and-paste' algorithm, introduced by Lal (1969) for the simulation of self-avoiding walks in the canonical ensemble, proved to be sufficient for this study. The algorithm was studied in detail by Madras and Sokal (1988) who called it the pivot algorithm. A version of the algorithm which proved effective for simulating polygons in the cubic lattice was invented by Madras *et al* (1990). The necessary elementary moves for the algorithm include several elements of the octahedral group, the symmetry group of the cubic lattice. Two pivots are chosen uniformly on the polygon and a symmetry operation is carried out on the shorter of the two segments connecting the pivots, as in Janse van Rensburg and Whittington (1991).

Although the probability that a polygon of length n is knotted approaches unity exponentially rapidly with increasing n (theorem 2.1), the knot probability is very small for intermediate values of n (up to about 2000 edges). It is therefore a considerable challenge to compute reliable values for the knot probabilities in confined spaces, where inefficient sampling by the algorithm may hamper reliable estimates. In addition, the knot probability depends strongly upon the quality of the solvent (Janse van Rensburg and Whittington 1990). We may simulate the quality of the solvent by introducing a monomer–monomer interaction between vertices in the polygon: if there are c nearest-neighbour contacts in a conformation, then we associate a reduced energy $-c\beta$ with the polygon. A Metropolis-style implementation of this effect is particularly easy, and works well over a fairly wide range of values of β. (Increasing positive values of β correspond to decreasing solvent quality.)

Knots in polygons can be detected by computing the value of the Alexander polynomial $\Delta(t)$ at $t = -1$ (Volodogskii *et al* 1974, Janse van Rensburg and Whittington 1990). If $|\Delta(-1)| \neq 1$ then the polygon is a knot. Otherwise we assume that it is the unknot. In fact the Alexander polynomial is not a perfect invariant, and is unable to distinguish every knot type. For instance the prime knot 8_{11} has the same Alexander polynomial as the composite knot $3_1\#6_1$, and 8_{15} has the same Alexander polynomial as $3_1\#7_2$. In this paper we are not concerned with distinguishing pairs of knots but only with deciding if a knot is non-trivial, and no knot with ten or less crossings has a trivial Alexander polynomial. However, the first problem does occur for us at ten crossings, since we only calculate $|\Delta(-1)|$ and not the full polynomial, and there are two knots with ten crossings which have $|\Delta(-1)| = 1$. Previous work (see, for instance, Janse van Rensburg and Whittington (1990)) has shown that knots with ten or more crossings are extremely rare, so we are confident that the error made in neglecting knots with $|\Delta(-1)| = 1$ will be insignificant.

Programming efficiency of the algorithms was maintained by using hash-coding (Knuth 1973, Horowitz and Sahni 1976). For every state sampled in the Markov chain we computed $\Delta(-1)$, the mean square radius of gyration R_n^2, the spans in the three lattice directions, L_χ, where $\chi = x, y$ and z, and the number of monomer–monomer contacts c. Rejection techniques for computing averages depending on L were implemented by reading the subsequence of states with $L_\chi \leqslant L$ and determining weighted averages over the three directions x, y and z. This procedure worked well for moderate to large values of L, but produced increasingly uncertain data as L was decreased to lower and lower values. We were indeed interested in the limiting behaviour of the knot probability as $L \to 1$, but could not determine these values from our data. Consequently, we developed an algorithm which was specifically designed for the case $L = 1$.

The algorithm is as follows. Let ω be a polygon in a 1-slab. Select two distinct vertices ω_i and ω_j on ω with uniform probability. ω_i and ω_j divide ω into two segments; choose the shorter of these. A pivot on this segment is an action of the octahedral group which either leaves ω_i and ω_j unchanged, or interchanges them. The details are as described in Madras *et al* (1990). One move which can always be attempted (since it interchanges ω_i and ω_j) is an *inversion* (a reflection through the midpoint of the line-segment connecting ω_i and ω_j). We must consider the effect of this inversion with three possible choices of pivots: (i) ω_i and ω_j are both in the $z = 0$ plane, (ii) ω_i and ω_j are both in the $z = 1$ plane, or (iii) ω_i is in the $z = 0$ plane while ω_j is in the $z = 1$ plane (or the interchange of this). In case (i), any vertex with z-component equal to 1 will be reflected outside the 1-slab to a vertex with z-component equal to -1. In this case we perform an additional reflection of the segment through the plane $z = 0$; this restores these vertices so that they again have z-components equal to 1. This elementary move is obviously reversible: select ω_i and ω_j again and perform an inversion followed by a plane reflection. We deal with case (ii) in an analogous manner. Case (iii) is trivial. We call this move an *adapted inversion*. For other moves (corresponding to other elements of the octahedral group) we may either reject any move which takes vertices outside the 1-slab or, in some cases, we can use the above trick (of a second reflection) to keep the segment in the slab. (Note that this trick does not work for L-slabs with $L > 1$, as one can easily check.) The proof of ergodicity follows the same general lines as that of Madras *et al* (1990).

This algorithm was coded using the same techniques as set out above. Runs were performed under the same conditions as above and the same data were collected. In this case, however, rejection techniques were not necessary in analysing the data.

It is possible to prove the ergodicity of a cut-and-paste type algorithm in a $(1, 1)$-prism, using exactly the arguments mentioned for the 1-slab. However, it is not necessary to compute the knot probability, since both intuitive and rigorous arguments show that no polygon in a $(1, 1)$-prism can be knotted (see the appendix).

4. Numerical results

In this section we present our numerical results for the incidence of knots in lattice polygons on the simple cubic lattice, with the polygons confined in slabs or prisms. We run the algorithm for mN attempted pivot transformations, where we determined the knot type of N polygons, with each observation separated by m attemped transformations. We choose $N = 50\,000$, with $m = 50$ for polygons in a good solvent and $m = 200$ for polygons in a poor solvent to compensate for the decrease in the acceptance rate of the algorithm with deteriorating quality of the solvent.

To present error bars for our estimates it was necessary to calculate the autocorrelation times in our MC simulations, using the techniques developed by Madras and Sokal (1988). In subsection 4.1 we consider the knottedness of polygons in a good solvent, and we consider the effects of a poor solvent in subsection 4.2.

4.1. The knot probability for polygons in a good solvent

Polygons confined in a slab

It is reasonable to expect an increase of the knot probability of polygons in an L-slab with decreasing L; the confined polygons become smaller in size and are more likely to be knotted (Janse van Rensburg and Whittington 1990). However, it is not at all clear whether this trend will continue as L tends to 1. In figure 1 we show the knot probability as a function of L for polygons of lengths $n = 600$, 800, 1200 and 1600 confined in slabs of different widths. For each fixed n the probability appears to reach a maximum for a finite value of $L = L(n)$ and the fraction of knotted polygons decreases with L if $L < L(n)$. To confirm the existence of the maxima at $L = L(n)$, we computed the knot probability at $L = 1$ using the 1-slab pivot algorithm as set out above. We found a knot probability which is almost zero for every n. The presence of a maximum in the probability may reflect the competition between the higher probability for a polygon with smaller radius of gyration to be knotted, and the difficulty of forming knots in confined geometries due to the steric interactions in the polygon. If the polygon is squeezed along a given axis to a width L, then it spreads in the other directions, thus increasing the mean-square radius of gyration again, and one expects a decrease in the fraction of knotted configurations.

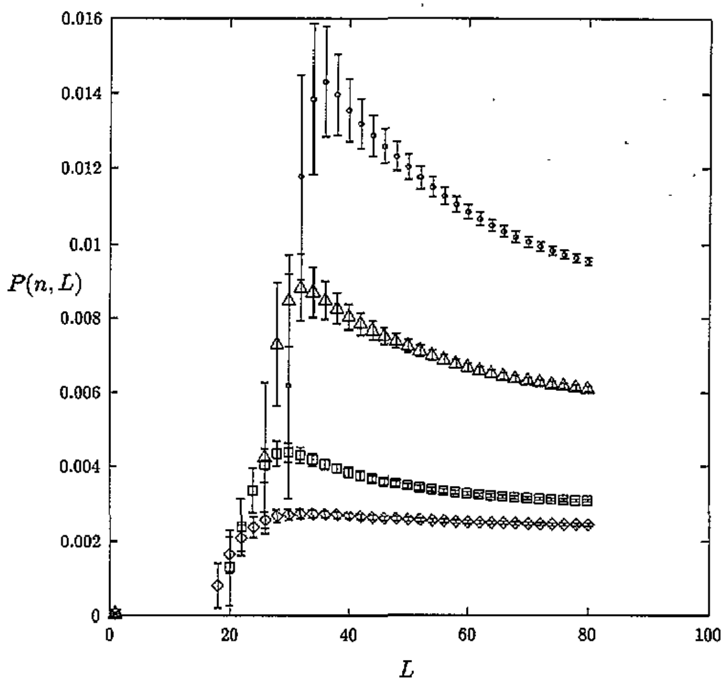

Figure 1. Plot of the knot probability $P(n, L)$ versus L for polygons of different sizes n ($n = 600$ (◇), $n = 800$ (□), $n = 1200$ (△), $n = 1600$ (○)) confined in slabs of width L.

Equation (2.3) suggests that the fraction of unknotted conformations in an L-slab, $P^0(n, L)$, behaves as

$$P^0(n, L) \simeq \mathcal{A}\, \mathrm{e}^{-\alpha(L)n}\,. \tag{4.1}$$

In figure 2 we plot $\ln P^0(n, L)$ as a function of n for $L = 40, 50, 60$. The straight lines shown are the fits obtained from a weighted least-square linear regression. This linear behaviour supports (4.1); moreover it is clear that the value of $\alpha(L)$ increases as L decreases. If we take the error bars to be three standard deviations, and if we discard points corresponding to polygons of small size, i.e. with $n = 600$, we obtain the following values for α: $\alpha(L = 40) = (1.23 \pm 0.20) \times 10^{-5}$, $\alpha(L = 50) = (1.07 \pm 0.16) \times 10^{-5}$ and $\alpha(L = 60) = (9.5 \pm 1.4) \times 10^{-6}$.

In figure 3 we plot the mean-square radius of gyration against L for different values of n. For fixed n, each curve has a minimum for approximately the same $L = L(n)$ for which the knot probability reaches its maximum. This observation supports the idea that knottedness in polygons is closely correlated with the 'size' of the conformation: the more compact the polygon, the more likely it will be knotted. Moreover, the polygons in the 1-slab have very large mean-square radii of gyration, and we observe a low knot probability.

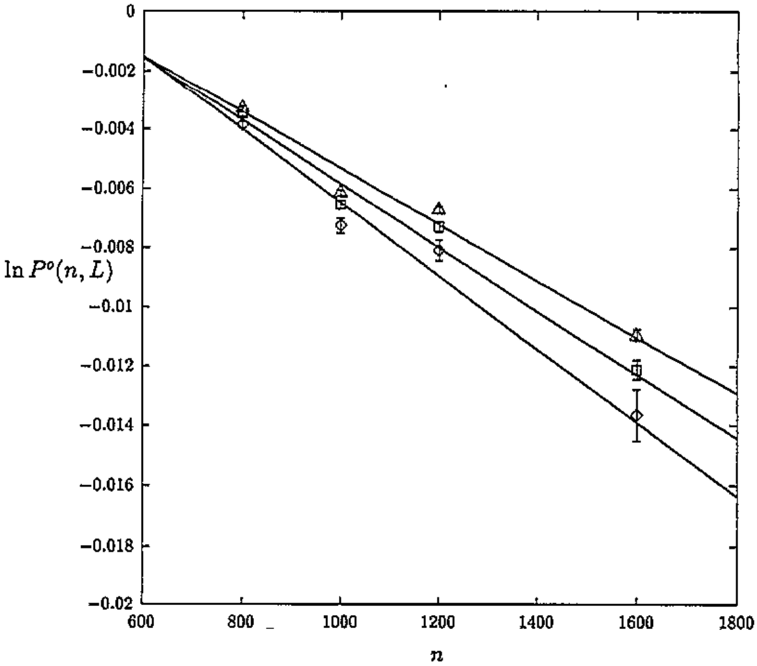

Figure 2. Plot of $\ln P^0(n, L)$, for a polygon in a slab, against n for three fixed values of L ($L = 40$ (◇), $L = 50$ (□), $L = 60$ (△)). The full lines are least-squares fits.

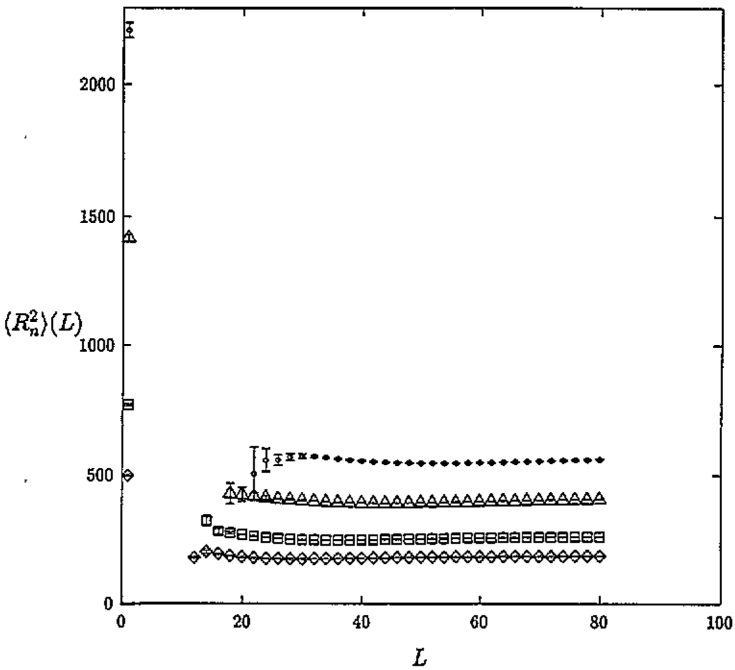

Figure 3. Plot of $\langle R_n^2 \rangle (L)$ versus L for different values of n ($n = 600$ (◇), $n = 800$ (□), $n = 1200$ (△), $n = 1600$ (○)).

Polygons confined in a prism

We performed the same kind of analysis for polygons in an (L, L)-prism. In this case the polygon fits into the prism if L_a and L_b are both less than L, with $a = x, b = y$, or $a = x, b = z$, or $a = y, b = z$. Weighted averages in three directions were taken to compute means over the ensemble of polygons by rejection techniques.

In figure 4 we plot the knot probability as a function of L for different values of n. We see exactly the same kind of behaviour found in the case of the slab. The only difference is in the values of the maxima, which are considerably higher than in the slab case; in a prism a polygon is more confined, and therefore more compact, and we expect a higher probability of being knotted.

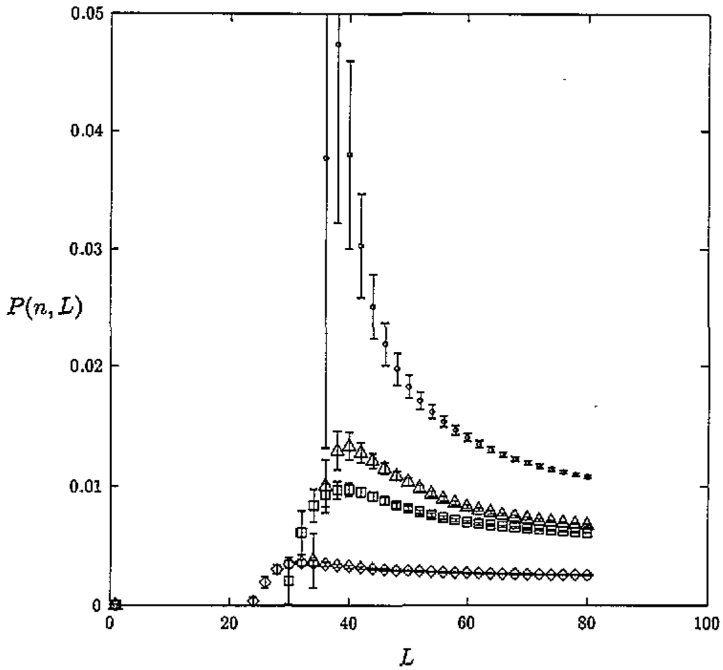

Figure 4. Plot of the knot probability $P(n, L)$ versus L for polygons of different sizes n ($n = 600(\Diamond), n = 800(\Box), n = 1200$ ($\triangle$), $n = 1600$ ($\circ$)) confined in prisms of width $L \times L$.

In figure 5 we plot $\ln P^0(n, L)$ as a function of n for three different fixed values of L ($L = 40, 50, 60$), and we also give the curves obtained from a weighted linear regression. There is a clear dependence of α on L: $\alpha(L = 40) = (2.25 \pm 0.30) \times 10^{-5}$, $\alpha(L = 50) = (1.70 \pm 0.15) \times 10^{-5}$ and $\alpha(L = 60) = (1.29 \pm 0.15) \times 10^{-5}$. The mean-square radius of gyration exhibits a minimum at approximately the value of L where the knot probability has a maximum.

4.2. *Incidence of knots in a poor solvent*

Since the effect of a poor solvent is to increase the knot probability, in this situation we expect all the features observed in the previous section, but with higher knot probability. We choose for the parameter β the value $\beta = 0.26$ since it is known (Janse van Rensburg

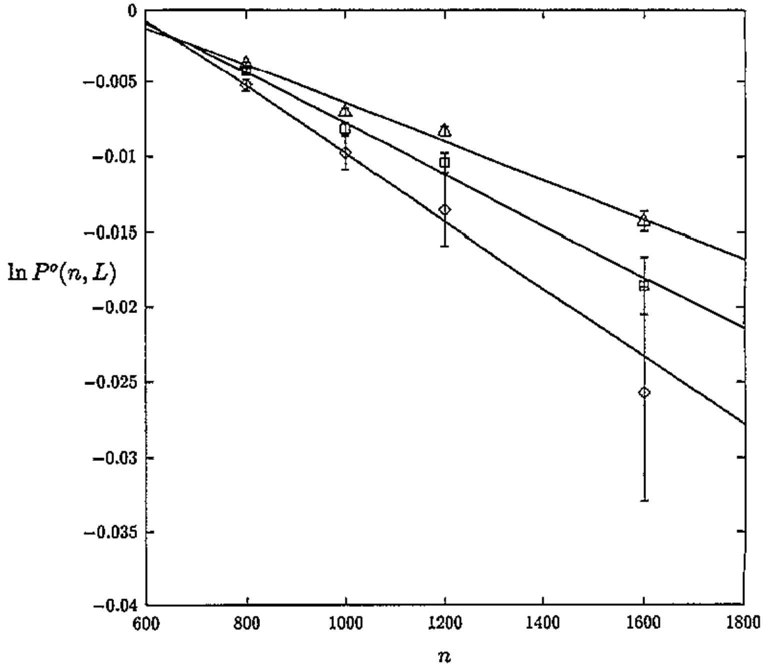

Figure 5. Plot of $\ln P^0(n, L)$, for a polygon in a prism, against n for three fixed values of L ($L = 40$ (◇), $L = 50$ (□), $L = 60$ (△)). The full lines are least-squares fits.

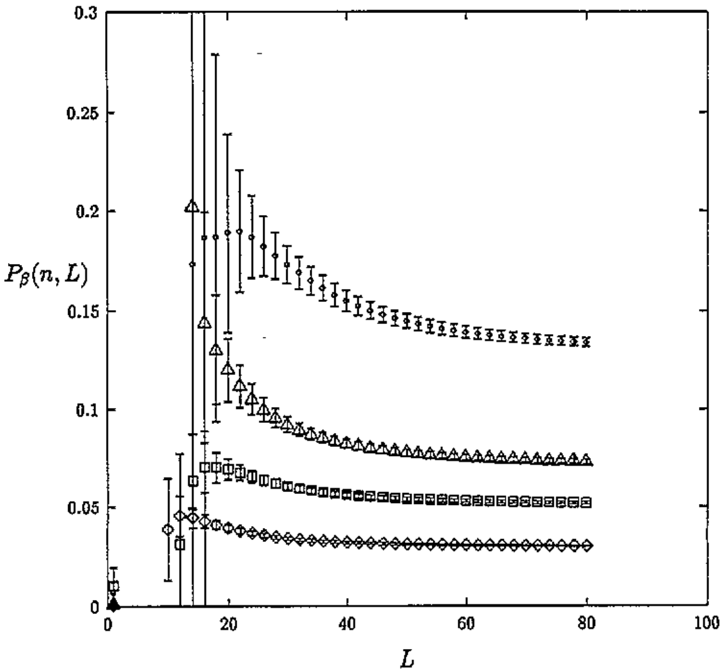

Figure 6. Plot of the knot probability $P_\beta(n, L)$ versus L for polygons of different sizes n ($n = 400$ (◇), $n = 600$ (□), $n = 800$ (△), $n = 1000$ (○)) confined in slabs of width L.

et al 1992) that this corresponds to a very poor solvent model for polygons in the simple cubic lattice. We performed all our analysis keeping β fixed at this value.

Polygons in a slab

In figure 6 we show the dependence of the knot probability on L for polygons of different sizes (n = 400, 600, 800, 1000) confined in slabs of different widths L. We considered polygons shorter than in the case of a good solvent model since the performance of the pivot algorithm is not as good in this regime as it is in a good solvent model. In particular, the autocorrelation times of the algorithm increase significantly with decreasing solvent quality. To compensate for this, we increased the number of attempted pivots between taking samples in the implementation of the algorithm. The general behaviour of the knot probability is the same as in the good solvent case, except that the values are higher: more polygons are knotted. This is to be expected, since the polygons are more compact in this regime, and we have seen that this correlates with a larger knot probability.

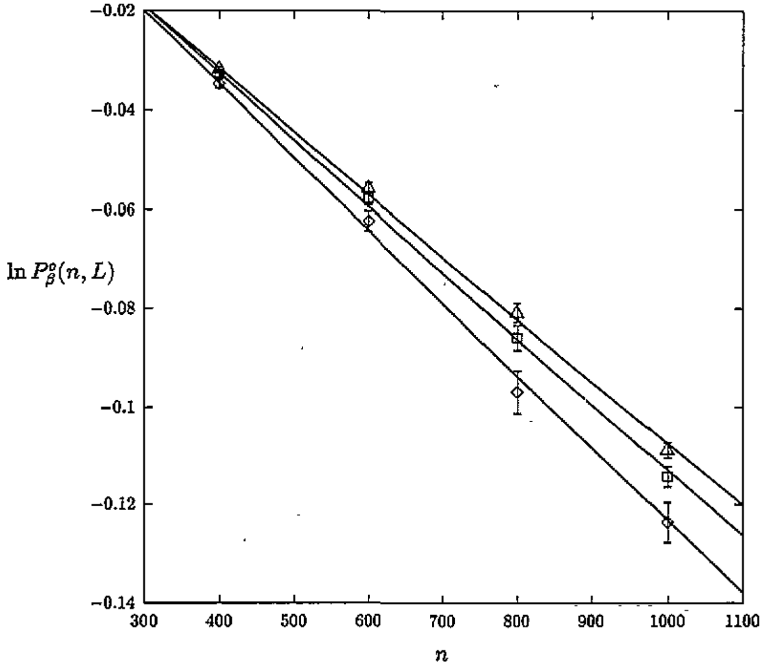

Figure 7. Plot of $\ln P^0_\beta(n, L)$, for a polygon in a slab, against n for three fixed values of L ($L = 30$ (◇), $L = 40$ (□), $L = 50$ (△)). The full lines are least-squares fits.

It is reasonable to assume for the knot probability of a polygon in a poor solvent a behaviour analogous to that of (4.1), where $\alpha = \alpha(L, \beta)$ now also depends on the quality of the solvent. In figure 7 we plot $\ln P^0_\beta(n, L)$ as a function of n for $L = 30, 40, 50$, and we include the lines obtained from a weighted least-squares linear regression. If we assume error bars which are three times the standard deviation, we obtain the following values for α: $\alpha(L = 30) = (1.475 \pm 0.050) \times 10^{-4}$, $\alpha(L = 40) = (1.340 \pm 0.033) \times 10^{-4}$ and $\alpha(L = 50) = (1.265 \pm 0.030) \times 10^{-4}$. Comparing these values with the ones obtained for slabs of the same L, in the good solvent regime, we clearly see the dependence of $\alpha(L)$ on the quality of the solvent. Similar trends were observed for polygons on the FCC lattice by

Janse van Rensburg and Whittington (1990). The mean-square radius of gyration behaves similarly to the good solvent case; here the more compact conformations result in smaller values of the mean-square radius of gyration.

Polygons in a prism
The same analysis was carried out for polygons in an (L, L)-prism. Again, the behaviour is similar to that of polygons in a prism in a good solvent regime, but with higher values for the knot probability.

We have analysed the n dependence of the knot probability at fixed values of L by assuming the functional form of (4.1), and we have obtained the following estimates of α from a weighted least-squares linear regression: $\alpha(L = 30) = (1.994 \pm 0.078) \times 10^{-4}$, $\alpha(L = 40) = (1.618 \pm 0.044) \times 10^{-4}$ and $\alpha(L = 50) = (1.431 \pm 0.033) \times 10^{-4}$. There is a clear dependence on L and the β dependence can be seen by comparing with the values obtained for polygons in good solvent. The mean-square radius of gyration exhibits a similar minimum as seen in the good solvent. This minimum corresponds to the value of L at which we have a maximum in the knot probability.

5. Discussion

We have shown rigorously that, for polygons confined to lie in a slab in $\mathbb{Z}^3$, the knot probability goes to unity exponentially rapidly as the size of the polygon increases. This is the same behaviour as for polygons in $\mathbb{Z}^3$. However, our numerical results show that geometrical constraints have a strong effect on the numerical values of the knot probability and that, as the width of the slab decreases, the knot probability goes through a maximum. Similar results are found numerically for polygons in a prism.

In addition, the quality of the solvent can have a large effect for polygons confined to slabs or prisms, just as for polygons in $\mathbb{Z}^3$. As the solvent becomes worse, the knot probability increases.

Of course, there are many interesting open questions. Can we say anything rigorously about the L-dependence of $\alpha(L)$? Is it possible to provide any rigorous results on the effect of solvent quality? In this work we have considered only two types of geometrical constraint. Certainly others are of interest and, in particular, it would be useful to have information on less regular constraints. In addition, although we are beginning to understand something about knotting in ring polymers, almost nothing is known about linking. This is an important area which has scarcely been addressed.

Acknowledgment

This work was financially supported by NSERC of Canada.

Appendix

We show that any polygon in a $(1, 1)$-prism is unknotted by proving that one can always reduce the length of the polygon, without changing its knot type, until we are left with a polygon of length four edges, and which is the unknot. The contruction proceeds by finding three edges which are arranged in a ⊔-conformation; we replace this by a single edge connecting the two endpoints. Trivially, this construction is an ambient isotopy if we think of the polygon as embedded in R^3. Suppose that the axis of the prism is parallel to the x-axis, and find the lexicographic top edge of the polygon. It is easy to see that this edge must be perpendicular to the x-axis; suppose without loss of generality that it points in the y direction. Let t be the top vertex (with x-component C), and let i, j and k be the three canonical unit vectors. Then we may denote $(t, -j)$ as the top edge, with endpoints t and $t - j$ in the plane $x = C$. The edges incident with the top edge are either parallel or perpendicular to each other. If they are parallel, then they must be of the form $(t, -k)$, and $(t - j, -k)$ or $(t, -i)$ and $(t - j, -i)$, respectively. In the first case we can replace the top edge and its neighbours by the single edge $(t - k, -j)$, and in the second case by $(t - i, -j)$, reducing the length of the polygon by two without changing its knot type. On the other hand, if the neighbouring edges are perpendicular, then they are $(t, -i)$ and $(t - j, -k)$, or $(t, -k)$ and $(t - j, -i)$. Without loss of generality, consider only the first of these. We argue now by exhausting all the possible cases. Incident with the second edge is either $(t - j - k, j)$ or $(t - j - k, -i)$. In the first case we find the sequence $(t, -j)$, $(t - j, -k)$, $(t - j - k, j)$, which we replace by $(t, -k)$, reducing the length of the polygon by 2 without changing its knot type. In the second case we we have $(t, -i)$, $(t, -j)$, $(t - j, -k)$, $(t - j - k, -i)$. Observe now that the vertex $(t - i - j)$ can only be occupied by a vertex of the polygon if either the edge $(t - i - j, j)$ or $(t - i - j, -k)$ is in the polygon (this follows, since every vertex in the prism has degree 4, and every vertex in the polygon has degree 2). But then we find one of the following sequences of edges: $(t - i - j, j)$, $(t, -i)$, $(t, -j)$, or $(t - i - j, -k)$, $(t - j - k, -i)$, $(t - j, -k)$. Both these are ⊔-conformations, and we can replace them by a single edge each. This exhausts all the possibilities. Continue this construction; eventually, we are left with a polygon consisting of only four edges, which is the unknot. Since we never changed the knot type of the polygon in this construction, the original polygon must be an unknot.

References

de Gennes P G 1984 *Macromol.* **17** 703

Dean F B and Cozzarelli N R 1985 *J. Biol. Chem.* **260** 4984

Diao Y 1990 On knotting of randomly embedded polygons in R^3 *PhD Thesis* Florida State University

Diao Y, Pippenger N and Sumners D W 1993 in preparation

Edwards S F 1967 *Proc. Phys. Soc.* **1** 15

—— 1968 *J. Phys. A: Math. Gen.* **91** 513

Frisch H L and Klempner D 1970 *Adv. Macromolecular Chem.* **2** 149

Hammersley J M 1961 *Proc. Camb. Phil. Soc.* **57** 516

Hammersley J M and Whittington S G 1985 *J. Phys. A* **18** 101

Horowitz E and Sahni S 1976 *Fundamentals of Data Structure* (Potomac, MD: Computer Science Press)

Janse van Rensburg E J and Whittington S G 1990 *J. Phys. A: Math. Gen* **23** 3573

—— 1991 *J. Phys. A: Math. Gen* **24** 3935

Janse van Rensburg E J, Sumners D W, Wasserman E and Whittington S G 1992 *J. Phys. A: Math. Gen* **25** 6557

Kendall W S 1979 *J. London Math. Soc.* 2 **19** 378

Kesten H 1963 *J. Math. Phys.* **4** 960

Knuth D E 1973 *The Art of Computer Programming* vol 3 (Reading, MA: Addison-Wesley)

Koniaris K and Muthukumar M 1991 *J. Chem. Phys.* **95** 2873

Lal M 1969 *Mol. Phys.* **17** 57

Madras N and Slade G 1993 *The Self-avoiding Walk* (Boston: Birkhäuser)

Madras N and Sokal A D 1988 *J. Stat. Phys.* **50** 109

Madras N, Orlitsky A and Shepp L A 1990 *J. Stat. Phys.* **58** 159

Michels J P J and Wiegel F W 1986 *Proc. R. Soc.* A **403** 269

—— 1989 *J. Phys. A: Math. Gen.* **22** 2393

Pippenger N 1989 *Discrete Appl. Math.* **25** 273

Shaw S Y and Wang J C 1993 *Science* **260** 533
Soteros C E, Sumners D W and Whittington S G 1992 *Math. Proc. Camb. Phil. Soc.* **111** 75
Soteros C E and Whittington S G 1989 *J. Phys. A* **22** 5259
Sumners D W and Whittington S G 1988 *J. Phys. A: Math. Gen.* **21** 1689
Vologodskii A V, Lukashin A V, Frank-Kamenetskii M D and Anshelevich V V 1974 *Sov. Phys.–JETP* **39** 1059
Wasserman S A and Cozzarelli N R 1986 *Science* **232** 951
—— 1991 *J. Biol. Chem.* **266** 20567
Wasserman S A, Dungan J M and Cozzarelli N R 1985 *Science* **229** 171